Journal of Magnetic Resonance 200 (2009) 29–37

Contents lists available at ScienceDirect

Journal of Magnetic Resonance

journal homepage: www.elsevier.com/locate/jmr

High-frequency EPR applications of open nonradiative resonators

G. Annino [a,*], M. Fittipaldi [b,1], M. Martinelli [a], H. Moons [b], S. Van Doorslaer [b], E. Goovaerts [b]

[a] Istituto per i Processi Chimico-Fisici, CNR, via G. Moruzzi 1, 56124 Pisa, Italy
[b] Departement Natuurkunde, Universiteit Antwerpen, Universiteitsplein 1, B-2610 Antwerpen, Belgium

ARTICLE INFO

Article history:
Received 3 February 2009
Revised 30 April 2009
Available online 29 May 2009

Keywords:
High-frequency EPR
Single-mode resonator
Open resonator
Electron-spin-echo
ELDOR-detected NMR
ODMR
Submillimeter wavelengths
ENDOR

ABSTRACT

A new class of open single-mode cavities, the nonradiative (NR) resonators, has recently been proposed in order to overcome the limitations of standard cylindrical cavities and Fabry-Perot resonators at millimeter wavelengths. This paper presents the first applications of a NR resonator in W-band pulsed electron paramagnetic resonance spectroscopy. It consists of a cylindrical cavity having a lateral aperture that represents about 35% of its total height. Electron-spin-echo measurements performed on different samples show that the signal-to-noise ratio and the optimal pulse length obtained with the proposed device are comparable to those obtained with the closed cavity used in the commercial W-band spectrometer, at both cryogenic and room temperature. Similar results have been obtained for paramagnetic species optically activated by means of an optical fiber inserted in the aperture of the resonator. The insertion losses estimated for the probe employed with the NR resonator are higher than those of the commercial probe, hence, demonstrating that the proposed cavity holds the promise of improved resonator performance.

1. Introduction

In electron paramagnetic resonance (EPR), the highest absolute sensitivity for samples with low and moderate losses is expected to be obtained by the use of single-mode resonators, where the active region of the device is of the order of the resonant wavelength [1,2]. At W-band and higher frequencies, the state-of-the-art in terms of minimum detectable number of spins and shortest π-pulse length is given by the cylindrical metallic cavity operating in the TE_{011} mode [3–13]. The basic structure of the cavity is represented by a cylindrical volume delimited by metallic walls and plungers [14]. One of the simpler excitation configurations of this resonator is based on a small coupling hole [15]. The size of the hole is chosen to permit a complete transfer of energy from the external feeding system to the resonator – the so-called critical coupling – for common working conditions. As a rule, the coupling between source and resonator increases with the diameter of the coupling hole and decreases with the thickness of the wall in which the hole is drilled. However, a hole with small diameter is preferable in order to minimize the perturbation of the resonance mode. The ideal coupling hole should thus have a diameter and, consequently, a thickness that is much smaller than the resonant wavelength. For microwave radiation at standard EPR wavelengths, these constraints do not pose serious difficulties, whereas at millimeter wavelengths they can become critical. A typical coupling hole for a W-band TE_{011} cavity has a diameter of 0.8 mm and thickness less than 50 μm [3]. The construction of the cavity is often complicated by a series of thin slits, necessary for radiofrequency or optical excitation of the sample. The height of the slits must also be much smaller than the employed wavelengths. At W-band frequencies, the slits have a typical height and mutual distance of ca. 0.2 mm [3,4]. Therefore, the rescaling of this design to shorter wavelengths is not trivial. Even when these difficulties have been overcome by the adoption of ingenious technical solutions, the results do not satisfy theoretical expectations [9,16].

Many of the complications related to the construction of a cylindrical cavity are avoided using Fabry-Perot resonators. However, this is achieved at the expense of lower filling factors and sensitivities. The magnetic field generated in these open multi-mode devices is also considerably weaker than that obtainable with the cylindrical single-mode cavity [3,4,9,17–19].

At centimeter wavelengths, there have been several studies dedicated to the construction of single-mode resonators with an open structure, such as the slotted tube resonator [20] and the loop-gap resonator (LGR) [21]. Rescaling to W-band frequency and beyond such devices poses similar problems as for the standard cylindrical cavity, due both to the complexity of their structure and their expected relatively low performance. For instance,

* Corresponding author. Fax: +39 050 3152236.
E-mail addresses: geannino@ipcf.cnr.it (G. Annino), maria.fittipaldi@unifi.it (M. Fittipaldi), massimo@ipcf.cnr.it (M. Martinelli), hans.moons@ua.ac.be (H. Moons), sabine.vandoorslaer@ua.ac.be (S. Van Doorslaer), etienne.goovaerts@ua.ac.be (E. Goovaerts).
[1] Present address: INSTM, Dipartimento di Chimica, Università di Firenze, via della Lastruccia 3, 50019 Sesto Fiorentino, Italy.

1090-7807/$ - see front matter © 2009 Elsevier Inc. All rights reserved.
doi:10.1016/j.jmr.2009.05.011

in the case of the most sophisticated LGR, the absolute W-band sensitivity is expected to be comparable to that of a cylindrical TE_{011} cavity with relatively modest quality factor [22]. An extensive discussion of the basic characteristics of open single-mode resonators proposed for EPR applications can be found in the popular treatise by Poole [23].

The above considerations, together with the recent impetus in the development of high-frequency EPR spectrometers operating over the entire millimeter wavelength range, have stimulated the search for novel single-mode resonators.

Open resonators based on the concept of a nonradiative (NR) structure have been demonstrated to be a valid alternative to the standard single-mode cavities [16,24,25]. In the context of electromagnetic devices, a NR structure can be defined as an active region of similar size to the employed wavelength λ, shielded by a metallic surface having large apertures. In contrast to closed cavities, where the apertures which permit external excitation of samples are as small as possible in order to avoid significant redistribution of the modal fields, the aperture in a NR structure represents an essential element for the field distribution and confinement properties. The constraint limiting aperture size to be much smaller than λ does not apply to NR structures, where it can be comparable to the resonant wavelength [16]. Despite the largely open character of the structure, the NR configurations can support trapped (i.e. nonradiating) modes. Such modes can be isolated, namely placed in the frequency spectrum below the cutoff of the modes propagating away from the structure, or embedded in a continuous spectrum of propagating modes. In the latter case, the trapped mode is usually decoupled from the propagating modes by symmetry reasons, such as opposite parity with respect to a symmetry plane [26]. An *ante litteram* version of a NR cavity was presented early in the 70's within the framework of optically detected magnetic resonance (ODMR) studies at X-band and Q-band [27–29].

Since in a NR configuration the apertures are essential features of the structure, they cannot be considered (and treated) as perturbations. The design of the cavity and the calculation of its modal field must take into account the final open structure. As a general rule, it is possible to demonstrate that the NR resonators can support trapped modes with field distribution similar to that of the TE_{011} mode of the closed cylindrical cavity. This is the case for structures with rotational invariance, which are indeed compatible with transverse electric (TE) modes [16].

Amongst the possible NR structures, the TE_{011} mode resonator, resembling a cylindrical cavity split into two parts, has been already proved competitive at millimeter and submillimeter wavelengths [30]. In this device, the limiting height of the aperture is $\frac{\lambda_0}{2}$, with λ_0 the resonant wavelength, whereas the overall size of the resonator is of the order of λ_0 [31]. Hence, this resonator combines the minimum active volume typical of a single-mode cavity with a largely open structure resembling a Fabry-Perot resonator. Moreover, the open structure simplifies the excitation of the resonator, minimizing the distortion of the modal fields. It also permits radiofrequency and optical irradiation of the sample without the need of a modified design.

In the work presented here, the open NR cavity has been employed in W-band pulse EPR measurements. We discuss the results obtained compared to those for a commercial closed cavity. In particular, we demonstrate that the development of NR resonators, while not yet completely explored, is at a mature stage and ready for state-of-the-art application at millimeter and submillimeter wavelengths.

The arguments treated in the paper are organized as follows. Section 2 introduces the essential theoretical aspects at the base of the proposed device. Section 3 describes the resonator. The electromagnetic characteristics of the resonator and of the overall experimental set-up are discussed in Section 4. Several types of EPR measurements on different samples are discussed in Section 5, together with the performance of the resonator in each case. Finally, in Section 6 some conclusions and an outline of the directions for further development of NR resonators are given.

2. General aspects

The structure of the NR resonator is shown schematically in Fig. 1a, where the pink shaded regions represent the volume accessible to the radiation. The cyan shaded regions represent the movable plungers. The axial cross-section and dimensions of the resonator are shown in Fig. 1b.

The cavity is composed of two parallel metallic plates kept at the distance l, having coaxial holes of radius r. The holes are closed by plungers, whose relative distance is indicated by l'. The distance of the holes from the closest side of the plates is indicated by t.

Neglecting the finite lateral extension of the plates, the structure of Fig. 1a has rotational invariance about the longitudinal axis of the cavity. It supports therefore transverse electric modes with no azimuthal dependence. These modes can be generically indicated as TE_0^c modes, where the superscript c refers to the cavity. Consider now a hypothetical TE_0^c mode trapped in the central volume of the cavity. Such a mode cannot transfer energy to the

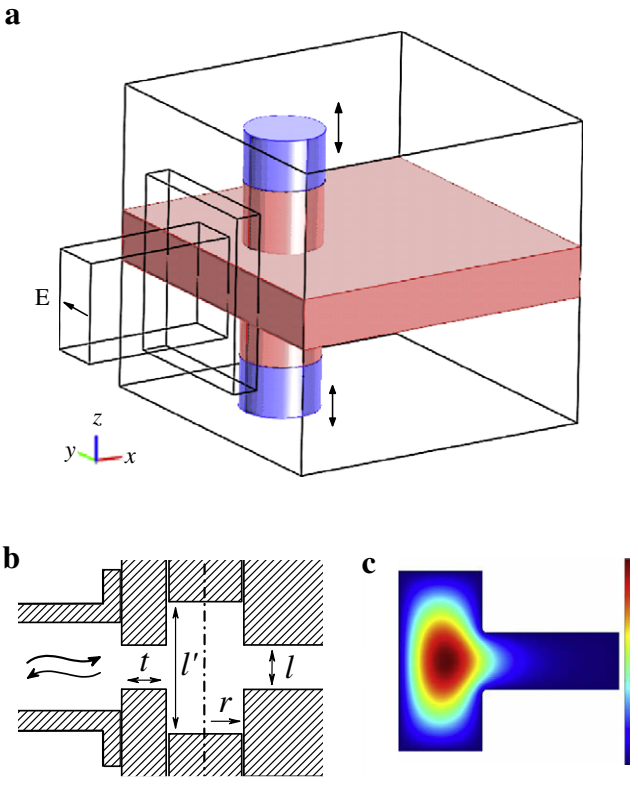

Fig. 1. (a) Schematic three-dimensional view of the proposed NR resonator and of the excitation waveguide. The polarization of the electric field of the incoming radiation is also shown. The pink shaded region indicates the volume accessible to the radiation. The cyan shaded regions represent the mobile plungers. (b) Axial cross-section of the resonator and of the excitation waveguide, along the direction of the excitation waveguide. The dimensions of the cavity are indicated. The undulated arrows represent the incoming and the reflected radiation. (c) Azimuthal electric field of the TE_{011} mode in half of the axial cross-section of the resonator, calculated for a case in which $r = 1.9$ mm, $l' = 4.1$ mm, $l = 1.3$ mm, to which corresponds a resonance frequency of 93.96 GHz. The corner between the cylindrical waveguide and the parallel-plate waveguide has been rounded, with radius of curvature $r_r \sim 3 \times 10^{-2}\lambda_0$. (For interpretation of the references to colour in this figure legend, the reader is referred to the web version of this article.)

cutoff-less transverse electromagnetic (TEM) modes propagating along the plates, since the TE_0^c mode does not have common field components with the TEM modes [16,26]. The radiative decay of the TE_0^c mode requires a coupling with the TE_0^w modes propagating along the parallel-plate waveguide (indicated by the superscript *w*), whose cutoff λ_{cutoff} is given by

$$l = \frac{\lambda_{cutoff}}{2}. \quad (1)$$

When the resonant wavelength λ_0 of the TE_0^c mode is larger than λ_{cutoff}, namely when $l < \frac{\lambda_0}{2}$, such coupling vanishes and the TE_0^c mode behaves as a completely confined mode. A resonance with wavelength λ_0 can be obtained with cavities having dimensions of the order of λ_0. Accordingly, the maximum height *l* of the aperture in the open resonator of Fig. 1a can represent up to half of the cavity height (Eq. (1)).

The typical electric field distribution of the TE_{011} mode of the open NR cavity is shown in Fig. 1c for a case in which $\frac{2r}{l} \sim 0.93$ and $\frac{l}{l'} \sim 0.32$, as calculated with the finite-element software Multiphysics 3.4 (Comsol, Se). The sharp corner between the cylindrical waveguide and the parallel-plate waveguide has been rounded with radius of curvature $\frac{r_r}{\lambda_0} \sim 3 \times 10^{-2}$, in order to obtain a more realistic configuration.

The electric field distribution is qualitatively similar to that of the analogous mode of the closed cylindrical cavity, the main difference being in the field outside the cylindrical volume of the cavity. The fraction of the electromagnetic energy outside this cylindrical volume, and its decay length, can be controlled by varying *l*. In the case of Fig. 1, this fraction is about 11% of the total energy. Despite the large aperture of the structure, the mode is mainly confined inside the cylindrical volume. Outside this volume, the field decreases exponentially, because the region between the parallel plates is effectively a waveguide below the cutoff for the resonance mode. In the symmetry plane at a distance 2*r* from the axis of the resonator, the maximum amplitude of the electric field is about 4.9% of the maximum amplitude at a distance *r*, i.e. on the boundary of the cylindrical cavity, and about 2.7% of the absolute maximum. In the case considered, the finite lateral extension of the resonator becomes irrelevant when it is larger than twice the diameter of the cylindrical region. On the other hand, a reduced lateral extension of the cavity can be exploited to couple the resonator to an external feeding system. Such a situation is illustrated in Fig. 1a. Here, the cavity holes are drilled close to a side of the plates, where the excitation waveguide is placed. For a given level of coupling, the required length *t* (see Fig. 1b) of the excitation region between the cavity and the edge of the plates depends on the field structure of the waveguide and on the quality factor of the resonance [23]. In order to avoid a leakage of the incoming radiation along the plates, the polarization of the wave must be orthogonal to that of the TEM mode of the plates, as shown in Fig. 1a. In this manner, the radiation is completely reflected outside the resonance.

A practical solution to control the coupling level is to change the position of the waveguide relative to the active region of the cavity [32]. This excitation scheme does not require the use of any component with critically small dimensions, as shown in the next section.

In EPR applications, the essential figures of merit of the resonator are given by the unloaded quality factor Q_0 and by the power-to-field conversion factor $\bar{B} = \sqrt{\frac{\langle B^2 \rangle}{P}}$, where the brackets indicate the average over a period of the radiation, *B* the magnetic induction field, and *P* the power dissipated in the resonator. The signal-to-noise and the square root of the absolute sensitivity in the continuous wave measurements are indeed proportional to Q_0 and $\bar{B}$, respectively [23]. Similar general rules are difficult to establish for the various pulsed techniques, where it is, however, expected that $\bar{B}$ plays a predominant role [33–35]. On the other hand, the influence of these quantities on the time resolution of the spectrometer can be easily formulated. The quality factor is inversely proportional to the ringing time of the resonator, the main element in the dead time of the spectrometer, whereas the conversion factor is inversely proportional to the length of flipping pulses [23].

It can thus be concluded that, as a general criterion, the optimal Q_0 of a resonator corresponds to the maximum value compatible with the dead time of the spectrometer, whereas the highest possible value is desirable for the conversion factor. The performance of the proposed resonator will be assessed in terms of both these quantities.

3. Experimental set-up

The concepts discussed in Sect. II have been employed to design a cavity resonating around 94 GHz. The structure of the cavity is illustrated in Fig. 2. It is composed of two copper plates separated by a distance of 1.3 mm and holes of 3.8 mm diameter in each plate aligned coaxially. Movable copper plungers of 3.7 mm diameter are accommodated in the holes (Fig. 2). The sample holder is a standard fused quartz tube of 0.6 mm internal diameter and 0.84 mm external diameter, inserted in the cavity through a 0.9 mm hole

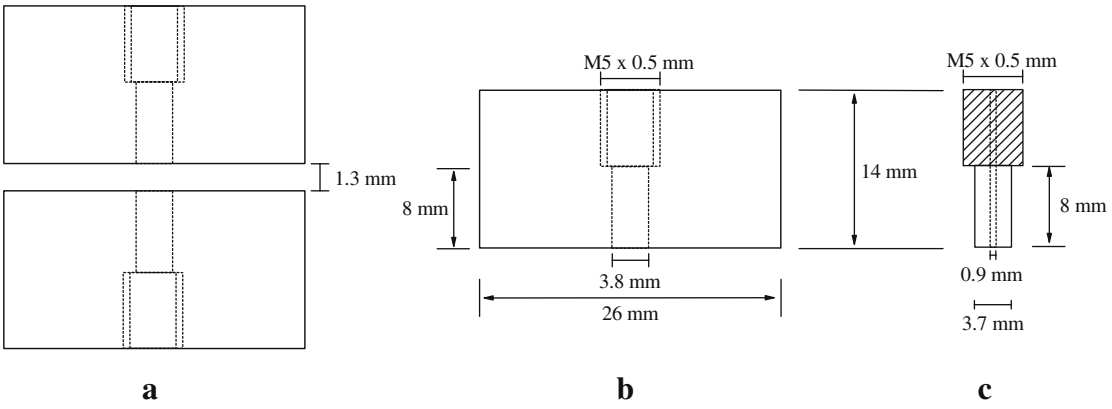

Fig. 2. Schematic representation of the 94 GHz resonator described in the text. (a) Side view of the two plates. The coaxial holes are indicated with dashed lines. (b) Detail of the single plate. The narrower part of the hole, which represents the cylindrical cavity, has a diameter of 3.8 mm. The initial part of the hole is threaded according to the M 5 × 0.5 mm mechanical standard. (c) Detail of the plunger and of its threaded region. The part of the plunger delimiting the resonant cavity has a diameter of 3.7 mm. A coaxial hole of 0.9 mm is drilled in the plunger, allowing the insertion of the sample holder.

drilled along the cylindrical axis in one or both plungers. The empty cavity resonates at 94 GHz for a distance of 4.1 mm between the plungers, in agreement with the numerical modeling. In the presence of a sample holder, for which a dielectric constant of $\varepsilon \sim 3.8$ is assumed, the same resonance frequency is obtained reducing the distance of the plungers to about 3.4 mm. In these working conditions, the lateral aperture of the cavity represents about 38% of its total height.

Fig. 3 shows the cavity, both as an exploded view (Fig. 3a) and a partially assembled view (Fig. 3b). The distance between the plates is blocked by an aluminum spacer on the back flange of the resonant assembly. The metallic surfaces surrounding the active region of the resonator were optically polished. The optimal length of the excitation region was found empirically, since the final quality factor of the mode was not known *a priori*. In the case considered, in which the radiation propagated along a WR-10 W-band waveguide, an adequate coupling level was obtained drilling the cavity at 1.4 mm from the boundary of the plates. The waveguide was oriented in order to have the electric field parallel to the plates, as shown in Fig. 1a. Such a configuration allowed critical coupling conditions to be achieved for all the investigated low-loss samples. The resonance frequency was controlled by the separation of the plungers.

4. Electromagnetic characteristics

The electromagnetic characteristics of the resonator were investigated by means of a custom-made microwave bridge working in the interval 93.18–95.26 GHz. Around 94 GHz, the typical quality factor close to critical coupling was $Q_L = 2700$ for the cavity having two plungers without the axial holes, which corresponds to an unloaded quality factor of $Q_{0,exp} = 5400 \pm 400$. The uncertainty of the latter value indicates the variability observed for different measurement conditions. The conversion factor for the axial field, defined as the root mean square of B_z in the point of maximum amplitude of the magnetic field, is calculated from the observed quality factor and from the field distribution of the resonance mode obtained from numerical modeling. For $Q_{0,exp} = 5400 \pm 400$, $\bar{B}_z = 14.3 \pm 0.5$ G/W$^{1/2}$. Such values can be compared with those of an ideal case, calculated considering only the ohmic losses in the conducting walls (copper resistivity: 1.724 μΩ cm), given by $Q_{0,th} = 7017$ and $\bar{B}_{z,th} = 16.35$ G/W$^{1/2}$. The difference between the observed and calculated values can be ascribed to the imperfect level of finishing of the surface of the resonator and to a residual irregularity in its geometric configuration. The difference increases when the plungers are drilled to accommodate the sample holder. In this case, $Q_{0,exp} = 4500 \pm 200$ and $\bar{B}_{z,exp} = 13.1 \pm 0.3$ G/W$^{1/2}$.

The theoretical figures of merit of the NR resonator can be compared also to those of a closed cylindrical cavity, which represents a natural term of comparison for the proposed device. The theoretical quality factor and conversion factor of a standard copper cavity with optimal aspect ratio are $Q^{cc}_{0,th} = 9759$ and $\bar{B}^{cc}_{z,th} = 19.38$ G/W$^{1/2}$, respectively. The high theoretical quality factor of a closed cylindrical cavity can be explained in terms of its higher active volume/surface ratio, since $Q_{0,th} = \frac{2}{\delta}\frac{\int_{vol} H^2 dV}{\int_{sur} H_t^2 dS}$, where δ is the skin depth in the conductor, H the magnetic field, H_t its component tangential to the conducting surface, and S the surface delimiting the active region of the resonator [14,36,37]. A comparison between the above conversion factors shows that

$$\frac{\bar{B}^{cc}_{z,th}}{\sqrt{Q^{cc}_{0,th}}} \simeq \frac{\bar{B}_{z,th}}{\sqrt{Q_{0,th}}}. \tag{2}$$

Such a property indicates that, despite its largely open structure, the active volume of the open NR resonator is very similar to that of the closed cavity and thus close to the minimal one. The conversion factor is indeed related to the active volume V of the resonator through the expression $\bar{B} = \sqrt{\frac{\langle B^2 \rangle}{P}} \propto \sqrt{\frac{W}{V \cdot P}} = \sqrt{\frac{Q_0}{\omega_0 \cdot V}}$, where W is the total electromagnetic energy stored in the cavity and ω_0 the angular resonance frequency [2,23]. Eq. (2) allows a rapid comparison between the conversion factor of a standard cavity and that of the NR resonator, once the related quality factors have been determined.

The presence of the sample holder reduces slightly the quality factor of the cavity ($Q_{0,exp}$) to ~4300 ± 200. The corresponding conversion factor is $\bar{B}_z = 16.6 \pm 0.4$ G/W$^{1/2}$, which is higher than that of the empty cavity due to the field concentration induced by the holder [23].

In the EPR set-up used here, the resonator was inserted at the end of a custom-made probe composed of part of a K-band waveguide joined at each end to part of a W-band waveguide through tapered regions. The overall length of this circuit is about 165 cm. The typical insertion losses of the probe operating around 94 GHz are of the order of 2.7 dB. The transmitted signal is also affected by standing waves having a periodicity of about 115 MHz and dynamics of about 7 dB.

EPR measurements with the NR resonator were made using a commercial W-band spectrometer (Bruker, Elexsys E680), combined with an Oxford Instruments superconducting magnet. The obtained results were compared with those obtained using the commercial probe head of the spectrometer, composed of a propagation circuit exciting a closed cylindrical TE_{011} cavity. The insertion losses of the probe at around 94 GHz are of the order of 1.5 dB.

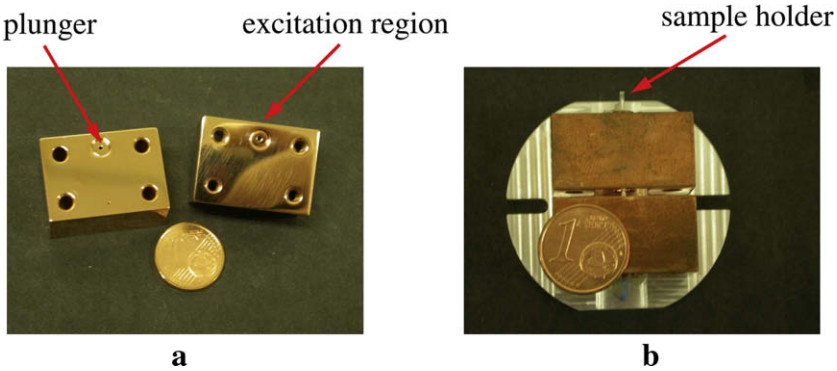

Fig. 3. (a) Plates composing the resonator, with arrows marking a plunger and the excitation region. (b) View of the assembled resonator, with the quartz sample holder inserted.

In this case, the standing waves have a periodicity of about 100 MHz and dynamics of about 1.3 dB.

The use of a resonator in variable measurement conditions requires a continuous control of the resonance frequency and of the level of the coupling, which can change due to mechanical relaxation or thermal drift. In the case of the NR cavity, the resonance frequency was fine-tuned moving only one of the plungers. The consequent asymmetry of the cavity with respect to its lateral aperture does not correspond to a similar asymmetry in the field distribution, as normally observed for standard TE_{011} cavities, where the maximum of the axial magnetic field is equidistant from the plungers. In the NR resonator described here, the lateral aperture acts as trapping element for the field, which tends to be locked to this aperture. Such behavior is illustrated in Fig. 4, which shows the axial magnetic induction field B_z along the axis of the resonator for two configurations with symmetric and non-symmetric plungers. The symmetric configuration corresponds to the cavity loaded by the sample holder, for a resonance frequency of 94.04 GHz. The distance between the plungers is here 3.4 mm. The removal of the sample holder increases the resonance frequency by 1.63 GHz. To re-establish the initial resonance frequency, it is necessary to displace one of the plungers by about 0.7 mm, as shown in Fig. 4. Despite the resulting large asymmetry of the structure, the maximum of the axial magnetic field experiences only a minimal displacement. A sample placed at the level of the aperture is subject to the maximum magnetic field in all the common working conditions, taking into account that the resonance frequency variation observed when lowering the temperature to cryogenic values is only about 300 MHz.

As described above, the coupling level can be adjusted moving the resonator with respect to the excitation waveguide. In our case, such a solution was unpractical. A more common alternative is to perturb the excitation region of the resonator, where the fields of both the resonance mode and the propagating wave overlap [23]. At W-band, the latter approach has been effectively implemented by the research group of Möbius [3]. In this approach, the excitation waveguide was slotted in order to accommodate a Teflon strip having a tapered profile and a silver plated tip. The level of the coupling was therefore controlled moving the plated tip around the coupling hole. A similar construction was adopted for the open resonator considered here. The terminal part of the W-band waveguide was longitudinally slotted along one of its largest sides. The width of this slit was about 0.5 mm. The strip was obtained using a Teflon foil (0.3 mm thick). The tip of the Teflon strip was coated with a silver paste. The size of the conducting tip was about 1 mm, whereas the typical length of the strip was about 15 mm. The strip was moved along the slit in the waveguide by means of a translation mechanism, as indicated in Fig. 5. With this solution, the critical coupling was easily obtained for the various measurements discussed in the next section. However, the strip introduced non-negligible insertion losses depending strongly on its shape, which can easily exceed 2 dB.

The structure of the probe head employed in this work is shown in Fig. 5a. Fig. 5b illustrates the mechanisms used to adjust the coupling level and the resonance frequency, both controlled from the top of the probe head. The plunger was rotated by means of an attached lever. The total displacement of the lever along the direction of the incoming radiation corresponds to rotation of the plunger by approximately 30°. The resulting variation of the length of the cavity was sufficient to compensate the variation of the resonance frequency observed for the measurement conditions used.

5. EPR results

The EPR measurements were performed on several representative samples in order to evaluate the performance of the resonator under different working conditions.

A first series of measurements was realized at room temperature on a powder of γ-irradiated calcium formate, which is a standard sample employed for dosimetry [38]. The insertion losses of the probe head were minimized removing the mechanism controlling the coupling level, which is not necessary for room temperature measurements. Fig. 6 shows the electron-spin-echo (ESE)-detected signal of the radical generated by the γ irradiation, together with the signal of the same sample obtained with the Bru-

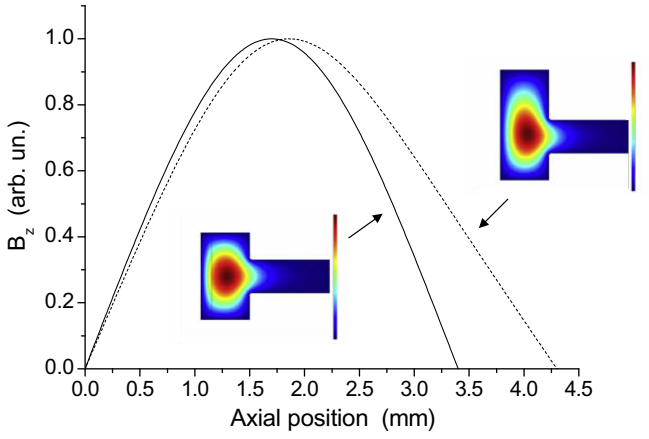

Fig. 4. Axial magnetic field B_z along the axis of the resonator for two different positions of the upper plunger and identical resonance frequency (see text). The zero of the abscissa axis refers to the lower plunger. The insets show the electric field distribution on half of the axial cross-section of the resonator for the two conditions, corresponding to the solid and dashed curves.

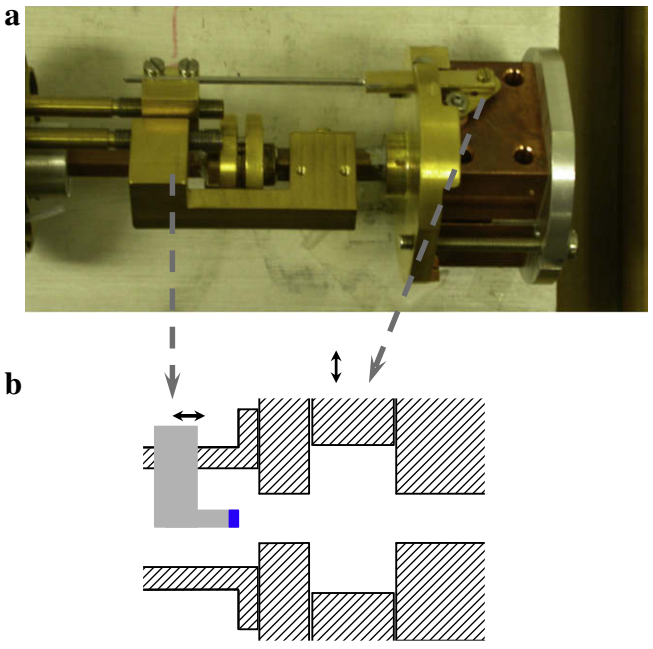

Fig. 5. (a) Detail of the probe head with the resonator and the mechanisms which control the resonance frequency and the coupling level. (b) Schematic drawing of the resonator and the excitation set-up (see also Fig. 1b). The dashed arrows link corresponding elements in the picture and the sketch. In particular, the arrow on the left links the mechanism controlling the coupling level and the sketch of the dielectric strip, the arrow on the right links the mechanism controlling the resonance frequency with the movable plunger. The solid arrows indicate the possible displacements of strip and plunger. The sample holder is not shown for the sake of clarity.

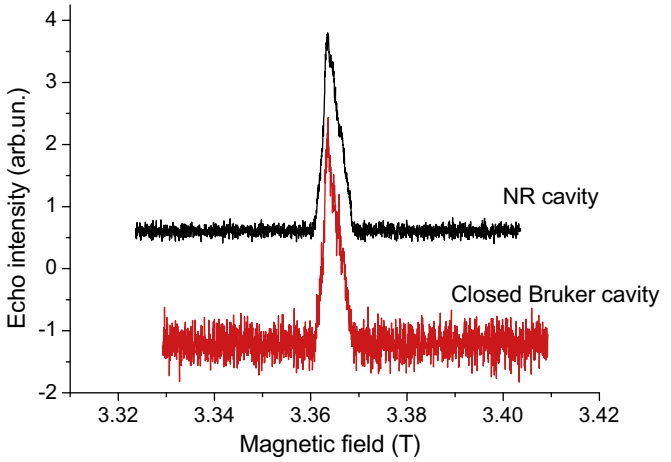

Fig. 6. Comparison between the electron-spin-echo-detected signal of the γ-irradiated calcium formate sample obtained with the NR resonator (black curve) and the Bruker cavity (red curve). Measurement parameters: $p_{\pi/2}$ = 188 ns, τ = 700 ns. The receiver gain was 24 dB (open cavity) 33 dB (Bruker cavity). (For interpretation of the references to colour in this figure legend, the reader is referred to the web version of this article.)

ker cavity. For both cavities, the parameters of the spectrometer were $\frac{\pi}{2}$ pulse length $p_{\pi/2}$ = 188 ns and a delay between pulses τ =700 ns. The receiver gain was 24 dB (open cavity) and 33 dB (Bruker cavity).

Fig. 7 shows the integrated intensity of the ESE signal as a function of the $p_{\pi/2}$ pulse length for a fixed microwave power.

On the basis of the curves reported in Figs. 6 and 7, the optimal pulse length for a given microwave power is the same for both resonators, while the signal-to-noise ratio is better by a factor 3 for the open cavity. This discrepancy can be qualitatively explained considering the different sample position inside the resonators. The sample holder extends along the entire height of the open cavity, whereas it can just touch the lower flat surface of the commercial cavity. In the latter case, the bottom sealing of the sample tube further reduces the active volume for the sample. Such differences can lead to diverse behavior of the optimal pulse length, related to the average of the field amplitude over the sample, and of the signal-to-noise ratio, related to the average of the field intensity. A more quantitative analysis would require a detailed knowledge of the structure of the commercial cavity.

The low temperature performance of the NR resonator was assessed measuring the ESE-detected EPR spectrum of a Cu(II)–octaethylporphyrin complex dissolved in chloroform [39]. The spectrum (at 20 K), recorded using the complete probe head shown in Fig. 5, is compared to that acquired using the commercial cavity in Fig. 8. The same optimal pulse parameters were used for both the measurements, $p_{\pi/2}$ = 188 ns, and τ = 800 ns, as well as the same receiver gain. In this case, the signal-to-noise ratios obtained for the two cavities are essentially the same. The analogous performance of the two resonators under these measurement conditions is attributed to the use of the mechanism controlling the coupling level in the NR probe head.

The performance of the open cavity at low temperatures was also investigated by measurements on a single-crystal sample by ELDOR-detected NMR [34,40]. Fig. 9 shows the ELDOR-detected NMR spectrum of the $[RhCl_6]^{4-}$ complex in AgCl single crystal [41,42], obtained at 5 K for an orientation close to that of the largest principal g-value. The ELDOR-detected NMR experiments were performed using the pulse sequence $(HTA)_{\nu 2}$-t_1-$(p_{\pi/2})_{\nu 1}$-τ-$(p_\pi)_{\nu 1}$-τ-echo, based on rectangular pulses [43]. HTA indicates a high turning angle pulse with variable microwave frequency (ν_2), whereas ν_1 indicates a fixed microwave frequency. t_1 and τ indicate the separation between the different pulses. The sequence used was composed by a $(HTA)_{\nu 2}$ pulse of 4 μs separated by 1 μs from the 480 ns $p_{\pi/2}$, which was separated by 1.52 μs from the 960 ns p_π. Another period τ of 1.52 μs separated the p_π pulse from the echo.

Several lines due to the hyperfine interactions with neighboring $^{35/37}Cl$, $^{107/109}Ag$ and ^{103}Rh nuclei can be observed in the 0–20 MHz region [42]. However, their detailed analysis is beyond the scope of this work.

The open structure of the NR resonator is particularly suited for illumination of the sample, which is essential for the study of paramagnetic species that are optically activated. The optical access to the sample can be simply obtained inserting an optical fiber between the plates of the resonator. The efficiency of the optical excitation increases reducing the distance between the fiber and the sample. However, a minimum distance must be kept in order to avoid perturbation of the cavity resonance. For the NR cavity, the TE_{011} mode is almost completely confined within 2 mm from

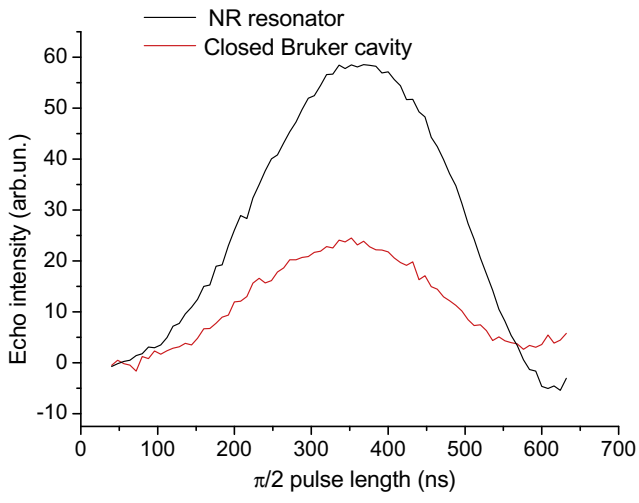

Fig. 7. Integrated intensity of the ESE signal versus $p_{\pi/2}$ for the NR resonator (black curve) and the Bruker cavity (red curve) for a given microwave power (different from the one used in Fig. 6). (For interpretation of the references to colour in this figure legend, the reader is referred to the web version of this article.)

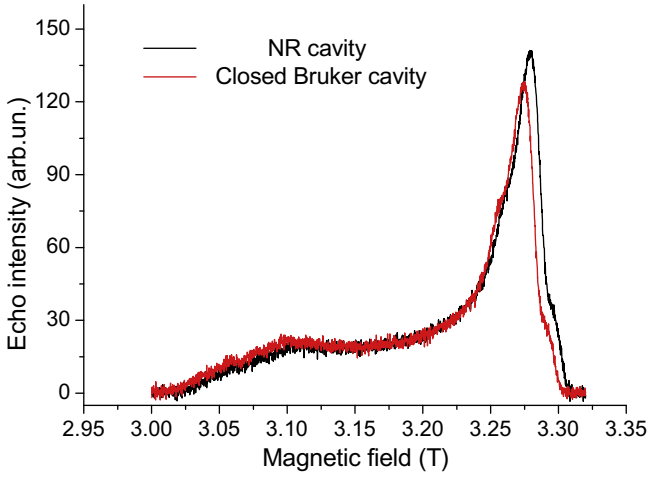

Fig. 8. ESE-detected signal of a frozen solution of Cu(II)–octaethylporphyrin in chloroform at 20 K obtained with the NR resonator (black curve) and with the Bruker cavity (red curve). Measurement parameters: $p_{\pi/2}$ = 188 ns and τ = 800 ns. The receiver gain was the same in both cases. (For interpretation of the references to colour in this figure legend, the reader is referred to the web version of this article.)

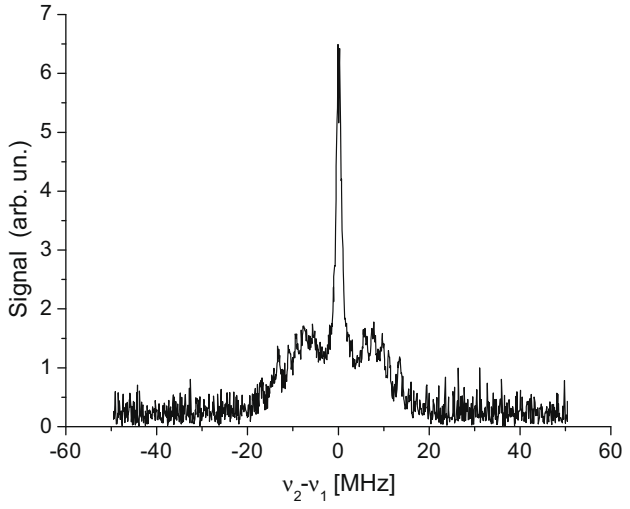

Fig. 9. ELDOR-detected NMR spectrum of the $[RhCl_6]^{4-}$ complex in AgCl single crystal at 5 K, measured in the NR cavity. Measurement parameters: static magnetic field B_0 = 2.7731 T, microwave frequency ν_1 = 94.042 GHz. The $(HTA)_{\nu 2}$-t_1-$(p_{\pi/2})_{\nu 1}$-τ-$(p_{\pi})_{\nu 1}$-τ-echo sequence (see text) was composed by the following time intervals: 4 μs-1 μs-480 ns-1.52 μs-960 ns-1.52 μs. The spectrum is an average of 3 scans.

the boundary of the cylindrical region. Beyond this distance, the resonator is insensitive to any extraneous element.

A similar experimental arrangement was employed for the room temperature characterization of the triplet state of pentacene molecules dispersed in a single crystal of *p*-terphenyl [44]. The ESE signal is shown in Fig. 10, together with that measured with a modified version of the Bruker probe head. In the latter case, excitation of the sample with nanosecond pulses from a frequency-doubled Q-switched Nd:YAG laser was performed by use of an optical fiber running through the long rod of the sample holder until it reaches the top of the quartz tube or rod carrying the sample [45]. The signal-to-noise ratios for the two cases, which also depend on the efficiency of the illumination, were essentially the same. In agreement with previous measurements, similar values of the optimal pulse lengths were also observed.

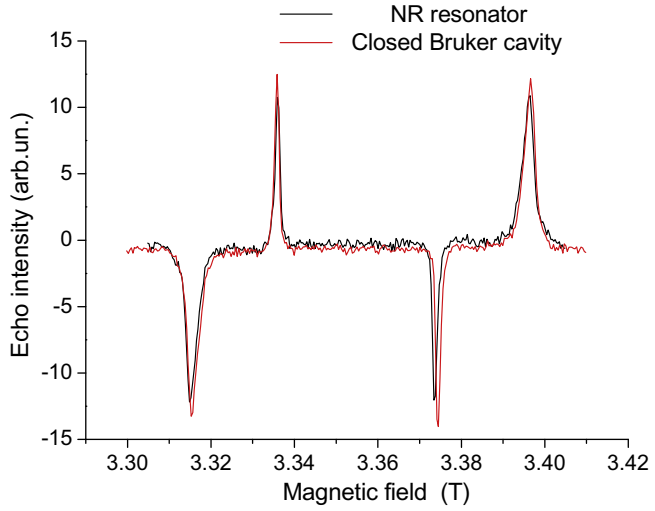

Fig. 10. ESE-detected signal of a pentacene-doped single crystal of *p*-terphenyl after nanosecond laser pulse excitation. The results obtained with the NR resonator and the commercial cavity are shown as black and red curves, respectively. The same measurement parameters were employed for both resonators. (For interpretation of the references to color in this figure legend, the reader is referred to the web version of this paper.)

The ease of lateral sample illumination, made possible by the NR resonator, is particularly advantageous in the study of opaque samples, where the number of paramagnetic centers generated by the light is expected to be proportional to the illuminated surface.

Another class of EPR techniques requiring the illumination of the sample is that of optically detected magnetic resonance (ODMR) [46]. The common feature of such techniques is that the resonance is observed as a variation of an optical signal (optical absorption or emission) from the sample. For photoluminescence intensity detected ODMR measurements, a requisite for a good sensitivity is the high efficiency in the collection of the emitted light. In the NR resonator, the light excitation can be obtained inserting an optical fiber along the sample holder, whereas a bundle of collecting fibers can be inserted between the parallel plates, almost completely encircling the active region of the resonator. The compact structure of the resonator allows the use of a reduced number of fibers, by which the emitted light can be collected with large solid angle coverage. Significant improvements can be expected in the ODMR detection by the use of NR resonators.

6. Conclusions and perspectives

The above comparative analysis demonstrates that, at W-band frequencies, the probe based on the NR resonator has similar or better performance than that of the commercial system based on a standard closed cavity. Taking into account the different insertion losses of the propagation circuits employed in the two resonators, this result shows that the performance of the NR resonator under different experimental conditions is better than that of the closed cavity provided with the spectrometer. Although the theoretical quality factor and conversion factor of the standard closed cavity appear to be better than those of the NR cavity, the figures of merit achievable at millimeter wavelengths can be easily superior for the NR resonator, due to its simple modular structure. The situation becomes even more favorable for such resonators, with respect to a standard open cavity based on thin slits, because of the additional losses introduced by such apertures.

These conclusions are supported by the indirect comparison with the single-mode cavities with the highest quality factor developed to date. At W-band, the highest merit factor (Q_0 = 7400) reported for a closed cavity is that of a TE_{011} gold cavity [13]. For most common materials the quality factor is not higher than Q_0 = 6000 [4], which is close to the value obtained in this work. The presence of the slits compromises significantly the merit factor, which is reduced to approximately Q_0 = 5000 or less [4,12,22], hence lower than the values obtained with the NR resonator described in this paper. It is worthwhile to note that lower quality factors, but better conversion factors, can be obtained with dielectric NR resonators [47].

At shorter millimeter wavelengths, the construction of a standard cavity becomes rather complex. On the contrary, the proposed resonator offers ample margins for miniaturization. The results reported herein suggest that submillimeter wavelength NR resonators can be produced using simple technology. Recent results have confirmed such expectations, a quality factor of Q_0 = 3300 at 285 GHz has been obtained for a resonator constructed following the same design concept, and promising preliminary results have been obtained for the same type of resonator at 350 GHz (Annino, unpublished results). These results compare well with the 275 GHz TE_{011} cavity built by the Leiden group [7,9]. In its closed version, this cavity exhibits a quality factor $Q_0 \simeq 3000$ [7], whereas the version including the slits for external irradiation reaches a merit factor $Q_0 \simeq 2000$ [9].

The benefits offered by the NR structure are not limited to the construction and performance of the resonator. Considerable improvements can also be made regarding the coupling control,

which suffered significant insertion losses in the investigated set-up. The origin of these losses is attributable to the long interaction region between the stripe and the mode propagating along the waveguide, which causes dielectric absorption and field distortion. On the other hand, the control of the coupling requires a field perturbation just in the excitation region, namely between the cylindrical cavity and the boundary of the plates. In the NR resonator this region is relatively extensive, 1.4 mm in the investigated system, and easily accessible. In principle, the excitation of the resonator can be effectively controlled inserting a dielectric strip in this region orthogonal to the propagating mode. Preliminary tests at W-band have shown that a dielectric strip with a tapered profile can change the coupling level from about 50% of the available power to beyond the critical coupling with negligible insertion losses.

The open structure of the NR resonator can be exploited in more complex experimental arrangements. In addition to the reported case of NR resonator enabling the rotation of the sample about two orthogonal axes [26], a NR cavity is currently under development for application in ENDOR spectroscopy. The preliminary results obtained with a slightly modified version of the resonator discussed in this paper show that the sample can be irradiated by a radiofrequency field with high efficiency, without influencing the microwave response of the resonator.

In conclusion, the design philosophy based on the NR structure solves the dichotomy which characterizes the present status of millimeter wavelength resonators, where the properties of the open Fabry-Perot cavities – simple but scarcely efficient – are at the opposite extreme to those of the closed single-mode resonators – efficient but complex to build. With their unique combination of simplicity, versatility, and high performance in different experimental conditions, the open NR resonators hold the promise of overcoming old problems and solving new challenges in high-field EPR spectroscopy.

Acknowledgments

The authors acknowledge the STSM program of the CNR, the Italian Ministero dell'Istruzione, dell'Università e della Ricerca, the COST action P15 'Advanced paramagnetic resonance methods in molecular biophysics', and the Fund of Scientific Research-Flanders (FWO) for their financial support. The precious technical support of Ivo Janssen is gratefully acknowledged as well. We are grateful to R. Bittl for the pentacene-doped *p*-terphenyl crystal. Finally, B.D. Howes is gratefully acknowledged for the critical reading of the article.

References

[1] Y.S. Lebedev, High-frequency continuous-wave electron spin resonance, in: L. Kevan, M.K. Bowman (Eds.), Modern Pulsed and Continuous-Wave Electron Spin Resonance, Wiley, New York, 1990, pp. 365–404.
[2] S.M. Spillane, T.J. Kippenberg, K.J. Vahala, K.W. Goh, E. Wilcut, H.J. Kimble, Ultrahigh-Q toroidal microresonators for cavity quantum electrodynamics, Phys. Rev. A 71 (2005) 013817.
[3] O. Burghaus, M. Rohrer, T. Gotzinger, M. Plato, K. Möbius, A novel high-field high-frequency EPR and ENDOR spectrometer operating at 3 mm wavelength, Meas. Sci. Technol. 3 (1992) 765–774.
[4] J.A.J.M. Disselhorst, H. Van der Meer, O.G. Poluektov, J. Schmidt, A pulsed EPR and ENDOR spectrometer operating at 95 GHz, J. Magn. Reson. A 115 (1995) 183–188.
[5] I. Gromov, V. Krymov, P. Manikandan, D. Arieli, D. Goldfarb, A W-band pulsed ENDOR spectrometer: setup and application to transition metal centers, J. Magn. Reson. 139 (1999) 8–17.
[6] V. Weis, M. Bennati, M. Rosay, J.A. Bryant, R.G. Griffin, High-field DNP and ENDOR with a novel multiple-frequency resonance structure, J. Magn. Reson. 140 (1999) 293–299.
[7] H. Blok, J.A.J.M. Disselhorst, S.B. Orlinskii, J. Schmidt, A continuous-wave and pulsed electron spin resonance spectrometer operating at 275 GHz, J. Magn. Reson. 166 (2004) 92–99.
[8] K. Möbius, A. Savitsky, A. Schnegg, M. Plato, M. Fuchs, High-field EPR spectroscopy applied to biological systems: characterization of molecular switches for electron and ion transfer, Phys. Chem. Chem. Phys. 7 (2005) 19–42.
[9] H. Blok, J.A.J.M. Disselhorst, H. van der Meer, S.B. Orlinskii, J. Schmidt, ENDOR spectroscopy at 275 GHz, J. Magn. Reson. 173 (2005) 49–53.
[10] E.P. Kirilina, T.F. Prisner, M. Bennati, B. Endeward, S.A. Dzuba, M.R. Fuchs, K. Mobius, A. Schnegg, Molecular dynamics of nitroxides in glasses as studied by multi-frequency EPR, Magn. Reson. Chem. 43 (2005) S119–S129.
[11] V.P. Denysenkov, T.F. Prisner, J. Stubbe, M. Bennati, High-frequency 180 GHz PELDOR, Appl. Magn. Reson. 29 (2005) 375–384.
[12] A. Schnegg, A.A. Dubinskii, M.R. Fuchs, Y.A. Grishin, E.P. Kirilina, W. Lubitz, M. Plato, A. Savitsky, K. Mobius, High-field EPR, ENDOR and ELDOR on bacterial photosynthetic reaction centers, Appl. Magn. Reson. 31 (2007) 59–98.
[13] A. Savitsky, A.A. Dubinskii, M. Plato, Y.A. Grishin, H. Zimmermann, K. Mobius, High-field EPR and ESEEM investigation of the nitrogen quadrupole interaction of nitroxide spin labels in disordered solids: toward differentiation between polarity and proticity matrix effects on protein function, J. Phys. Chem. B 112 (2008) 9079–9090.
[14] W.W. Hansen, A type of electrical resonator, J. Appl. Phys. 9 (1938) 654–663.
[15] H.A. Bethe, Theory of diffraction by small holes, Phys. Rev. 66 (1944) 163–182.
[16] G. Annino, M. Cassettari, M. Martinelli, A new concept of open TE_{011} cavity, IEEE Trans. Microwave Theory Tech. 57 (2009) 775–783.
[17] J.P. Barnes, J.H. Freed, Aqueous sample holders for high-frequency electron spin resonance, Rev. Sci. Instrum. 68 (1997) 2838–2846.
[18] I. Tkach, U. Rogulis, S. Greulich-Weber, J.M. Spaeth, W-band Fabry-Perot microwave resonators for optically detected electron paramagnetic resonance and electron nuclear double resonance of paramagnetic defects in solids, Rev. Sci. Instrum. 75 (2004) 4781–4788.
[19] J.M. Spaeth, I. Tkach, S. Greulich-Weber, H. Overhof, High-field optically detected EPR and ENDOR of semiconductor defects using W-band microwave Fabry-Perot resonators, Magn. Reson. Chem. 43 (2005) S153–S165.
[20] M. Mehring, F. Freysoldt, A slotted tube resonator (STR) for pulsed ESR and ODMR experiments, J. Phys. E 13 (1980) 894–895.
[21] W. Froncisz, J.S. Hyde, J. Magn. Reson. 47 (1982) 515.
[22] J.W. Sidabras, R.R. Mett, W. Froncisz, T.G. Camenisch, J.R. Anderson, J.S. Hyde, Multipurpose EPR loop-gap resonator and cylindrical TE011 cavity for aqueous samples at 94 GHz, Rev. Sci. Instrum. 78 (2007) 034701.
[23] C.P. Poole, Electron Spin Resonance: A Comprehensive Treatise on Experimental Techniques, Wiley, New York, 1983.
[24] G. Annino, M. Cassettari, M. Martinelli, High-frequency investigation on nonradiative single-mode dielectric resonators, Appl. Magn. Reson. 26 (2004) 447–456.
[25] S. Qi, K. Wu, Z. Oi, Hybrid integrated HEMT oscillator with a multiple-ring nonradiative dielectric (NRD) resonator feedback circuit, IEEE Trans. Microwave Theory Tech. 46 (1998) 1552–1558.
[26] G. Annino, M. Cassettari, M. Fittipaldi, M. Martinelli, High frequency single-mode resonators for EPR spectroscopy enabling rotations of the sample about two orthogonal axes, J. Magn. Reson. 176 (2005) 37–46.
[27] A. Wasiela, G. Ascarelli, Y.M. d'Aubigné, Optical detection of paramagnetic resonance of the self-trapped exciton in KBr, Phys. Rev. Lett. 31 (1973) 993–996.
[28] M. Chamel, R. Chicault, Y.M. d'Aubigné, A microwave cavity for EPR studies under light illumination, J. Phys. E 9 (1976) 87–88.
[29] K.M. Lee, Wall-less microwave cavity for optical detection of magnetic resonance, Rev. Sci. Instrum. 53 (1982) 702–704.
[30] G. Annino, M. Fittipaldi, M. Martinelli, S. Van Doorslaer, E. Goovaerts, Development and application of open single-mode resonators for high-frequency EPR, International Conference "Modern Development of Magnetic Resonance", Kazan, Russian Federation, 24–29 September 2007, Book of Abstracts, pp. 74–76.
[31] G. Annino, M. Cassettari, M. Martinelli, Open nonradiative cavities as millimeter wave single-mode resonators, Rev. Sci. Instrum. 76 (2005) 064702.
[32] G. Annino, M. Cassettari, M. Martinelli, P.J.M. van Bentum, A nonradiative approach to single-mode dielectric resonators, Appl. Magn. Reson. 24 (2003) 157–175.
[33] G.A. Rinard, R.W. Quine, J.R. Harbridge, R.T. Song, G.R. Eaton, S.S. Eaton, Frequency dependence of EPR signal-to-noise, J. Magn. Reson. 140 (1999) 218–227.
[34] A. Schweiger, G. Jeschke, Principles of Pulse Electron Paramagnetic Resonance, Oxford University Press, New York, 2001.
[35] A.P.M. Kentgens, J. Bart, P.J.M. van Bentum, A. Brinkmann, E.R.H. Van Eck, J.G.E. Gardeniers, J.W.G. Janssen, P. Knijn, S. Vasa, M.H.W. Verkuijlen, High-resolution liquid- and solid-state nuclear magnetic resonance of nanoliter sample volumes using microcoil detectors, J. Chem. Phys. 128 (2008) 052202.
[36] H.A. Atwater, Introduction to Microwave Theory, McGraw-Hill, New York, 1962.
[37] J.D. Jackson, Classical Electrodynamics, Wiley, New York, 1975.
[38] T.A. Vestad, E. Malinen, A. Lund, E.O. Hole, E. Sagstuen, EPR dosimetric properties of formates, Appl. Radiat. Isot. 59 (2003) 181–188.
[39] T.G. Brown, B.M. Hoffman, ^{14}N, ^{1}H, and metal ENDOR of single crystal Ag(II)(TPP) and Cu(II)(TPP), Mol. Phys. 39 (1980) 1073–1109.
[40] P. Schosseler, Th. Wacker, A. Schweiger, Pulsed ELDOR detected NMR, Chem. Phys. Lett. 224 (1994) 319–324.
[41] M.T. Olm, J.R. Niklas, J.M. Spaeth, M.C.R. Symons, Structure of a $(RhCl_6)^{4-}$ defect in AgCl, Phys. Rev. B 38 (1988) 4343–4351.

[42] H. Vrielinck, K. Sabbe, F. Callens, P. Matthys, Detection of charge compensating cation vacancies near Rh^{2+} complexes in AgCl and NaCl using Q-band ENDOR, Phys. Chem. Chem. Phys. 3 (2001) 1709–1716.
[43] M. Fittipaldi, I. Garcia-Rubio, F. Trandafir, I. Gromov, A. Schweiger, A. Bouwen, S. Van Doorslaer, A multi-frequency pulse EPR and ENDOR approach to study strongly coupled nuclei in frozen solutions of high-spin ferric heme proteins, J. Phys. Chem. B 112 (2008) 3859–3870.
[44] D.J. Sloop, H.L. Yu, T.S. Lin, S.I. Weissman, Electron spin echoes of a photoexcited triplet: pentacene in *p*-terphenyl crystals, J. Chem. Phys. 75 (1981) 3746–3757.
[45] G. Janssen, A. Bouwen, P. Casteels, E. Goovaerts, Implementation of optically detected magnetic resonance spectroscopy in a commercial W-band cylindrical cavity, Rev. Sci. Instrum. 72 (2001) 4295–4296.
[46] B.C. Cavenett, Optically detected magnetic resonance (O.D.M.R.) investigations of recombination processes in semiconductors, Adv. Phys. 30 (1981) 475–538.
[47] G. Annino, M. Cassettari, M. Martinelli, Axially open nonradiative structures: an example of single-mode resonator based on the sample holder, Rev. Sci. Instrum. 76 (2005) 084702.